

Zircaloy-4 Zr-Sn-Fe-Nb

High Temperature Deformation of Zircaloy-4 and Zr-Sn-Fe-Nb Alloy Cladding Tubes

, , *
220
* 494

Zircaloy -4 Zr - Sn - Fe - Nb
가 298~798K . Zr -
Sn - Fe - Nb Zircaloy - 4
Zircaloy - 4가 Zr - Sn - Fe - Nb . 250~400
가 Zircaloy - 4 Zr - Sn - Fe - Nb
, Zr - Sn - Fe - Nb .
. SEM , Zircaloy - 4 Zr - Sn - Fe - Nb
가 .

Abstract

In order to investigate the effect of dynamic strain aging on the high temperature deformation behavior of Zircaloy-4 and Zr-Sn-Fe-Nb nuclear fuel claddings, high temperature mechanical testing was carried out over the temperature range 298 ~ 798K. The strengths of Zr-Sn-Fe-Nb claddings were greater than those of Zircaloy-4 over the whole temperature range with the ductilities of Zr-Sn-Fe-Nb claddings slightly lower than those of Zircaloy-4. The plateau of the strength was observed in both Zircaloy-4 and Zr-Sn-Fe-Nb claddings although the plateau behavior was more pronounced in Zr-Sn-Fe-Nb claddings. The loss of the ductility associated with dynamic strain aging was observed in the same temperature range where the plateau was observed. SEM observation revealed that the fracture surfaces of both Zircaloy-4 and Zr-Sn-Fe-Nb claddings were ductile irrespective of strain rate and temperature. The predicted yield strength and elongation were in good agreement with the experimental data, supporting that the yield stress plateau and the ductility loss are associated with dynamic strain aging.

1. tube
UO₂ (pellet) tube¹⁾
,
. ,
가 300 400
(dynamic strain aging) (strain
rate sensitivity)²⁻⁵⁾
, 가 가 , , 가
가 1 2 가
. 가 , ,

5(a, c)

가

Hong⁶⁾

가

, Zircaloy-4

가 가

가

가

$$m = \frac{\ln(\hat{\sigma}_2/\hat{\sigma}_1)}{\ln(\hat{Y}_2/\hat{Y}_1)} \quad (1)$$

\hat{Y}_2 , \hat{Y}_1 \hat{Y}_1

E * ,

$$\hat{\sigma}_t = \hat{\sigma}_E + \hat{\sigma}^* + \hat{\sigma}_D = \hat{\sigma} + \hat{\sigma}_D \quad (2)$$

가 , D

6

plateau

6)

가

가

가

가

drag force가

가

가

가

가

가

D
가
D
plateau

6

6

가

(1)

가

가

가

$$s_D = s_D^o \exp\left\{-\frac{(T - \bar{T})^2}{B}\right\} \quad (1)$$

가 D 가 t 가 D *

2.10)

가

가

D

가

$$s_D = s_D^o \exp\left\{-\frac{(T - \bar{T})^2}{B}\right\} \quad (3)$$

B

s_D^o

가

, \bar{T}

가

가

D

가

D

plateau

⁹⁾ Hong^{6,9)}

Zircaloy-4

가

가

가 drag force \bar{T} , T_E Arrhenius-

$$\frac{1}{\bar{T}} = \frac{1}{T_E} = \frac{R}{Q} \ln A - \frac{R}{Q} \ln \dot{\epsilon} \quad (4)$$

(1) $\dot{\epsilon}$, $Q(=205\text{KJ mol}^{-1})^{(6)}$ Zircaloy-4, $A(=9.84 \times 10^{11})$ (2)

$$m_t = \frac{d\{\ln(\mathbf{s}^* + \mathbf{s}_D)\}}{d(\ln \dot{\epsilon})} = \frac{1}{\mathbf{s}^* + \mathbf{s}_D} \left\{ \mathbf{s}^* \frac{d(\ln \mathbf{s}^*)}{d(\ln \dot{\epsilon})} + \mathbf{s}_D \frac{d(\ln \mathbf{s}_D)}{d(\ln \dot{\epsilon})} \right\} = \frac{1}{\mathbf{s}^* + \mathbf{s}_D} (\mathbf{s}^* m^* + \mathbf{s}_D m_D) \quad (5)$$

m_t 가 , m^* , mD 가 가 ¹¹⁾ m^* 가 가 가 ¹²⁾ , m^* 가

$$m^* = \frac{d(\ln \mathbf{s}^*)}{d(\ln \dot{\epsilon})} = aT + b \quad (6)$$

$$\mathbf{s}^* = \mathbf{s}_o^* \left(\frac{\dot{\epsilon}}{\dot{\epsilon}_o} \right)^{aT+b} \quad (7)$$

\mathbf{s}_o^* $\dot{\epsilon}_o$

$$m_D = \frac{d(\ln \mathbf{s}_D)}{d(\ln \dot{\epsilon})} = \frac{d(\ln \mathbf{s}_D)}{d\bar{T}} \frac{d\bar{T}}{d(\ln \dot{\epsilon})} = \frac{2R(T - \bar{T})(\bar{T} - \Delta T)^2}{BQ} \quad (8)$$

(2)~ (8)

(2), (3) (7) Zircaloy-4 , \hat{a} , \hat{a} , \mathbf{s}_o^* , ΔT $\dot{\epsilon}_o$ $7.55 \times 10^{-5} \text{K}^{-1}$, -9×10^{-3} , $8.5 \times 10^2 \text{MPa}$, 38.9° $1.56 \times 10^5 \text{s}^{-1}$ 7 (2), (3) 가 3.33×10^{-3}

(7) plot . 250 350

가 plateau

9,12-14)

가

$$e_f(\%) = am_t + b \quad (9)$$

a(=1 × 10²) b(=12.9)

가가 , 가
 , 8
 (8) (9) Zircaloy-4 Zr-Sn-
 Fe-Nb 가 plateau가 ,
 가
 plateau 가
 , Hong¹⁵⁾ Zircaloy-4

4. Zircaloy-4 Zr-Sn-Fe-Nb

1. 가 250 400 가
2. Zircaloy-4 Zr-Sn-Fe-Nb
 Zr-Sn-Fe-Nb Zircaloy-4
3. plateau Zircaloy-4 Zr-Sn-Fe-
 Nb

Reference

1. J. H. Huang and S. P. Huang, J. Nucl. Mater., 208 (1994) 166
2. J. D. Lubahn, Trans. Metall. Soc. AIME., 185 (1949) 702
3. D. Lee, Metall. Trans., 1 (1970) 1607
4. A. M. Garde, E. Aigeltinger, B. N. Woodruff and R. E. Reed-Hill : Metall. Trans., 6A (1975) 1183
5. A. K. Miller and O. D. Sherby, Acta Metall., 26 (1978) 289
6. S. I. Hong, W. S. Ryu and C. S. Rim, J. Nucl. Mater., 116 (1983) 314
7. S. I. Hong, W. S. Ryu and C. S. Rim, J. Nucl. Mater., 120 (1984) 1
8. J. S. Song, S. D. Kim, S. I. Hong, Y. Choi and J. W. Kim, J. Kor. Inst. Met. & Mater., 35 (1997) 1668
9. S. I. Hong, Mater. Sci. Eng., 79 (1986) 1
10. S. I. Hong, Mater. Sci. Eng., 91 (1987) 137
11. S. I. Hong, Mater. Sci. Eng., 82 (1986) 175
12. R. E. Reed-Hill, Physical Metallurgy Principles, Van Nostrand, New York (1973) 348
13. R. W. Lund and W. D. Nix, Acta Metall., 24 (1973) 469
14. M. A. Burke and W. D. Nix, Acta Metall., 23 (1975) 793
15. S. I. Hong, Mater. Sci. Eng., 86 (1978) L1
16. C. J. McMahon, Mater. Sci. Eng., 42 (1980) 215

Table. 1 Chemical composition of Zr alloy

	Sn	Fe	Cr	Nb	O	Zr
Zircaloy-4	1.33	0.21	0.1	-	0.08	Bal.
Zr-Sn-Fe-Nb	0.7	0.74	-	1.1	0.13	Bal.

Figures caption

Fig. 1 Schematic configuration of tensile testing sample and grip.

Fig. 2 Variations in yield stress of Zircaloy-4(a) and Zr-Sn-Fe-Nb(b) nuclear fuel claddings.

Fig. 3 Variations in UTS of Zircaloy-4(a) and Zr-Sn-Fe-Nb(b) nuclear fuel claddings.

Fig. 4 Variations in elongations of Zircaloy-4(a) and Zr-Sn-Fe-Nb(b) nuclear fuel claddings.

Fig. 5 Fracture surfaces of Zircaloy-4(a, b) and Zr-Sn-Fe-Nb(c, d) nuclear fuel claddings. (a, c) room temperature, (b, d) 400

Fig. 6 Schematic flow stress versus temperature plots. The total flow stress σ consist of two separable parts.

Fig. 7 The predicted yield strength of Zircaloy-4 claddings plotted with the measured strength.

Fig. 8 The predicted elongation of Zircaloy-4 claddings plotted with the measured elongation.

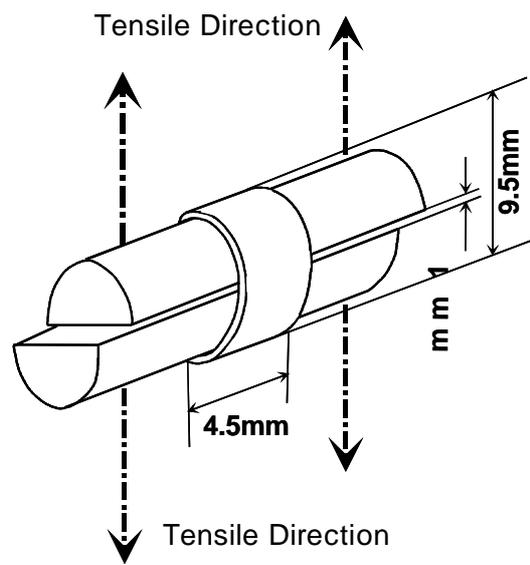
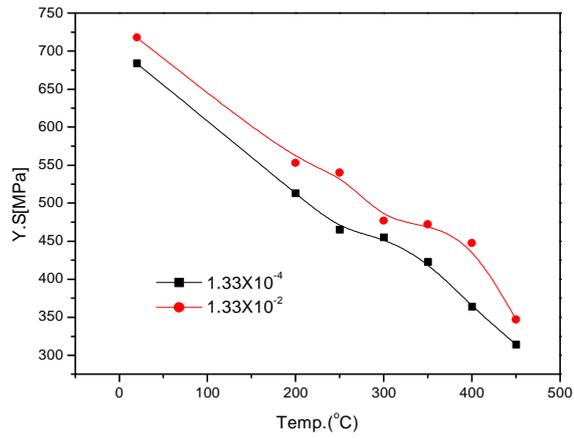
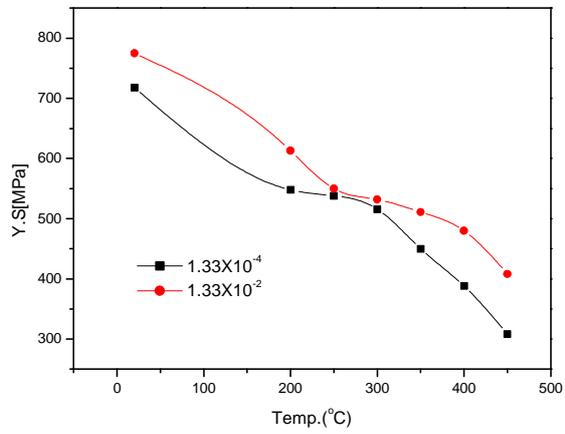


Fig. 1 Schematic configuration of tensile testing sample and grip.



(a)



(b)

Fig. 2 Variations in yield stress of Zircaloy-4(a) and Zr-Sn-Fe-Nb(b) nuclear fuel claddings.

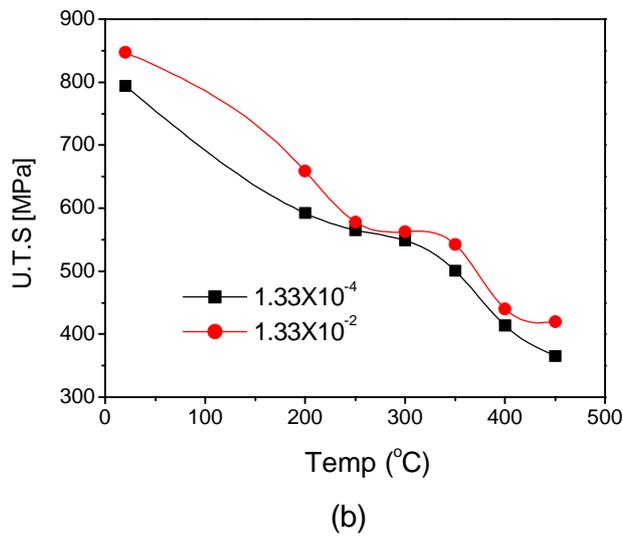
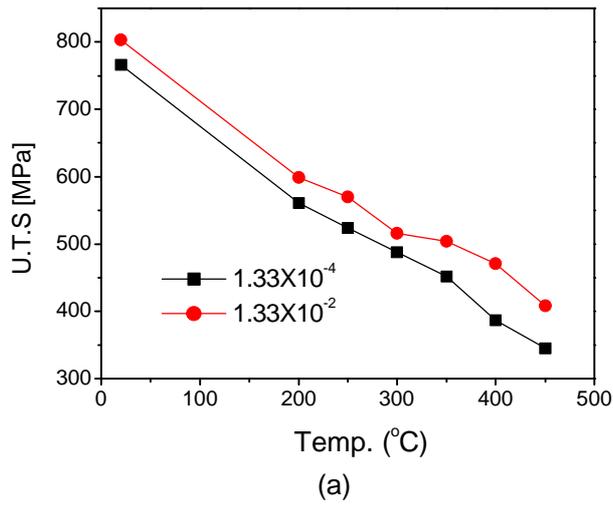
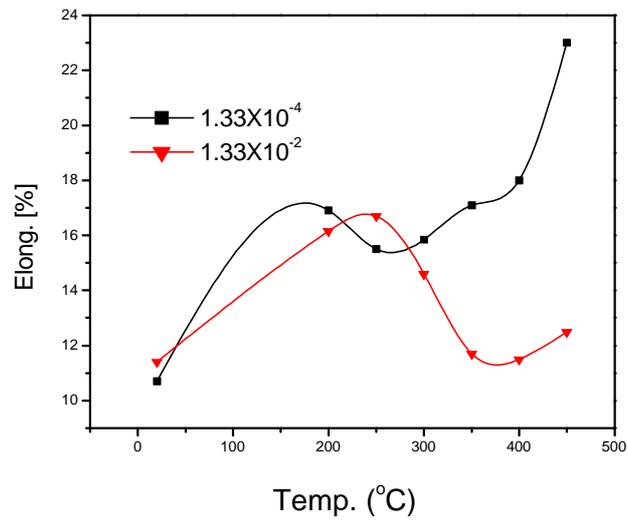
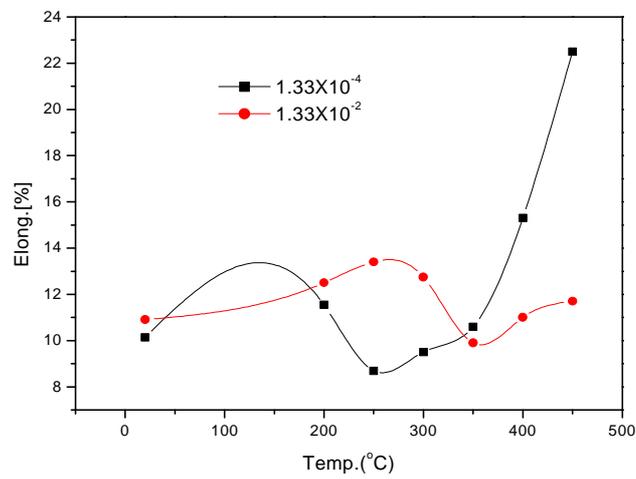


Fig. 3 Variations in UTS of Zircaloy-4(a) and Zr-Sn-Fe-Nb(b) nuclear fuel claddings.

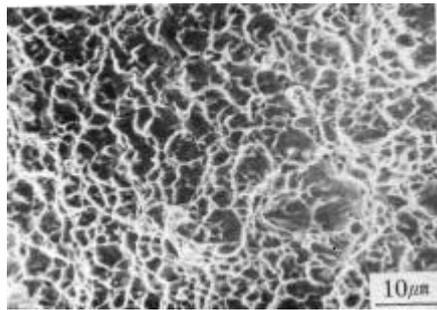


(a)

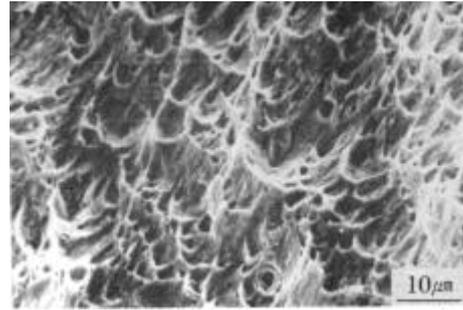


(b)

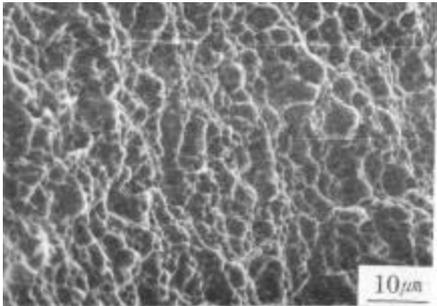
Fig. 4 Variations in elongations of Zircaloy-4(a) and Zr-Sn-Fe-Nb(b) nuclear fuel claddings.



(a)



(b)



(c)



(d)

Fig. 5 Fracture surfaces of Zircaloy-4(a, b) and Zr-Sn-Fe-Nb(c, d) nuclear fuel claddings. (a, c) room temperature, (b, d) 400

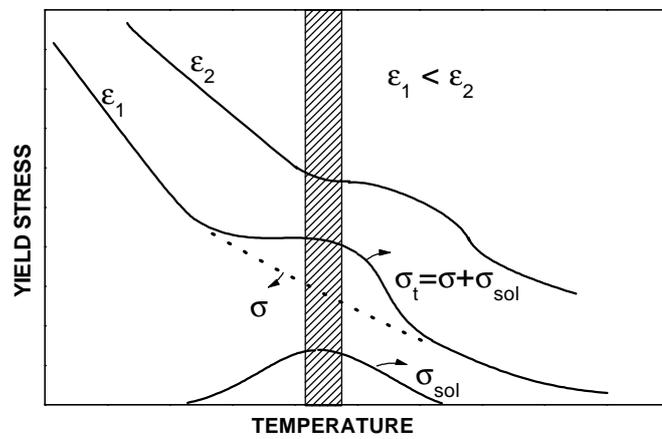


Fig. 6 Schematic flow stress versus temperature plots. The total flow stress σ_t consist of two separable parts.

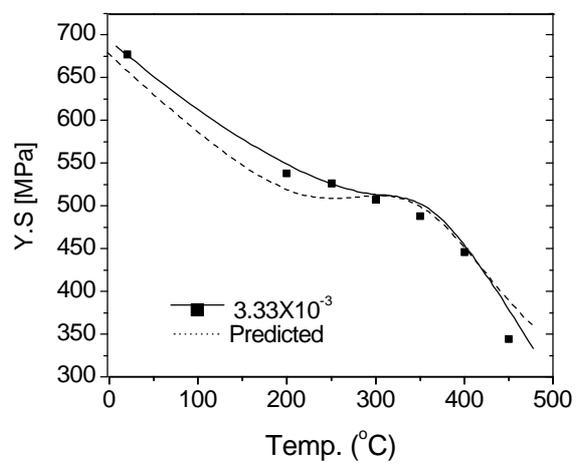


Fig. 7 The predicted yield strength of Zircaloy-4 claddings plotted with the measured strength.

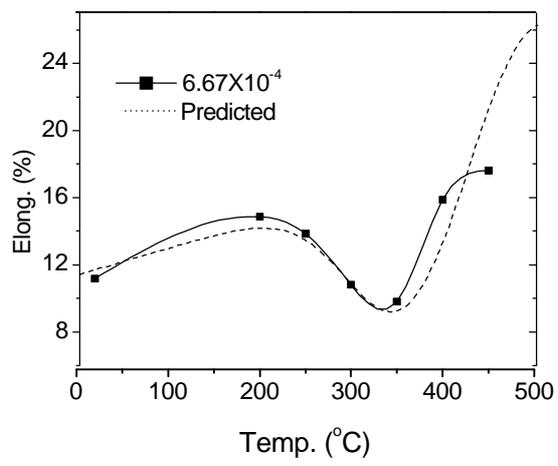


Fig. 8 The predicted elongation of Zircaloy-4 claddings plotted with the measured elongation.